Absorption spectrum of a two-level system subjected to a periodic pulse sequence

H. F. Fotso[1,2] and V. V. Dobrovitski[3,4]

[1]*Department of Physics and Astronomy, Iowa State University, Ames, Iowa 50011, USA*
[2]*Department of Physics, University at Albany (SUNY), Albany, New York 12222, USA*
[3]*Ames Laboratory, U.S. DOE, Ames, Iowa 50011, USA*
[4]*QuTech and Kavli Institute of Nanoscience, TU Delft, Lorentzweg 1, 2628 CJ Delft, Netherlands*

We investigate how the quantum control of a two-level system (TLS) coupled to photons can modify and tune the TLS's photon absorption spectrum. Tuning and controlling the emission and the absorption are of great interest, e.g., for the development of efficient interfaces between stationary and flying qubits in modern architectures for quantum computation and quantum communication. We consider periodic pulse control, where the TLS is subjected to a periodic sequence of the near-resonant Rabi driving pulses, each pulse implementing a 180° rotation. For small interpulse delays, the absorption spectrum features a pronounced peak of stimulated emission at the pulse frequency, similar satellite peaks with smaller spectral weights, and the net absorption peaks on the sides. As long as the detuning between the carrier frequency of the driving and the TLS transition frequency remains moderate, this spectral shape shows little change. Therefore, the pulse control allows shifting the absorption peak to a desired position and locks the overall absorption spectrum to the carrier frequency of the driving pulses. A detailed description of the spectrum and its evolution as a function time, the interpulse spacing, and the detuning is presented.

I. INTRODUCTION

An interface between stationary and flying qubits that enables long-range entanglement between different quantum network nodes is essential for quantum information processing [1]. It is of particular importance for the solid-state qubits, such as quantum dots or color centers [2–15], which can be efficiently coupled to each other via photons and thus employed for quantum communications and distributed quantum information processing. However, the slow fluctuations in the environment of the solid-state qubits (e.g., the local strain and/or the local electric fields) constitute a lingering challenge because they unpredictably shift the optical transition frequency of the qubits [16,17]. This slow drift of the transition frequency (spectral diffusion) makes it difficult to achieve the precise matching between the photons originating from different qubits that is required for efficient entanglement. To mitigate the spectral diffusion problem, various methods have been proposed and successfully used [5–9,16,18–23], focusing primarily on the tuning of the emission spectrum and on improving the indistinguishability of the photons emitted from different qubits. In particular, it has been recently suggested [23] that application of a periodic sequence of the optical control pulses to a quantum emitter (a two-level system coupled to the electromagnetic radiation bath) can redirect most of the emission into a peak located at a preset target frequency (determined by the carrier frequency of the pulse driving field) and therefore can greatly improve the indistinguishability of the photons coming from different emitters.

At the same time, there is growing interest, accompanied by impressive progress [24–26], in long-range entanglement schemes based on the photon absorption, and theoretical developments that allow control and tuning of the absorption spectra have become timely and interesting. Correspondingly, a question arises whether the absorption-based entanglement

can also be improved using the pulse control of the emitters, i.e., whether the absorption spectrum of a two-level system (TLS) coupled to the radiation bath can be modified and tuned by the control pulses. In addition, the studies of absorption of a TLS subjected to an external control are of fundamental interest due to the intimate connection between emission and absorption [27]. For instance, if the TLS is continuously driven by a strong coherent laser field, then the TLS emission spectrum has an interesting three-peak structure, with two additional side peaks located at the frequencies $\pm\Omega_R$ (where Ω_R is the laser Rabi driving frequency), and the absorption spectrum of the same system also acquires additional structure, displaying regions of gain, corresponding to an amplification of the probing weak field instead of attenuation [28,29].

The emission spectrum of the pulse-controlled TLS exhibits similarities with the continuously driven TLS emission [23]: it has a central peak at the carrier frequency of the pulses ω_0, as well as the satellite peaks at $\omega_0 \pm \pi/\tau$, $\pm 2\pi/\tau$, ..., where τ is the interpulse distance. Thus, it is reasonable to expect that absorption also can be controlled with the periodic pulses and that the resulting absorption spectrum also has nontrivial features. In this work we study the absorption spectrum of a TLS driven by a periodic sequence of optical π pulses and examine its dependence on the pulse sequence period and the detuning of the emitter with respect to the pulse frequency (Fig. 1). We show that both expectations above are correct, and therefore, the pulse control indeed can be a useful tool for controlling and tuning the absorption spectrum of a TLS. Specifically, the absorption spectrum has a well-defined central feature that includes a pronounced dip (which corresponds to stimulated emission at the carrier frequency of the pulses) and two absorption peaks on the sides. The spectrum also exhibits satellite features, with smaller spectral weights. The overall shape of the absorption spectrum does not change much as long as the detuning Δ between the carrier frequency of the driving pulses and the TLS transition frequency remains
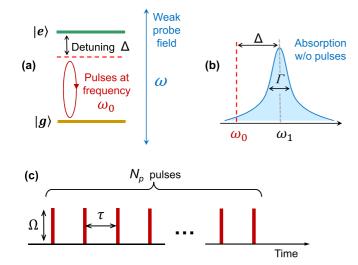
FIG. 1. (a) Schematic representation of the two-level system with ground state $|g\rangle$ and excited state $|e\rangle$ separated in the rotating frame by the detuning Δ. It is probed by measuring the energy absorbed from a weak field as a function of frequency. (b) The absorption spectrum in the absence of any driving field has a Lorentzian line shape centered around Δ. (c) We will evaluate the absorption spectrum when the system is driven by a periodic sequence of π pulses with interpulse time τ.

moderate ($\Delta \lesssim 1/\tau$) and as long as the value of τ is small in comparison with the spontaneous emission time. Therefore, we show that the optical control enables creation of pairs of quantum nodes (one node working as an emitter and the other as an absorber) with precisely matching frequencies and therefore greatly increased entanglement efficiency. This approach can also be used to improve the coupling of the emitters and the absorbers to optical cavities since the laser pulses can tune both the emission and the absorption lines of the respective quantum nodes, bringing them in resonance with the respective cavities and stabilizing both the emission and the absorption peaks at the desired location.

The rest of this paper is organized as follows. In Sec. II we describe the model of the two-level system coupled to the photon bath and controlled by the pulses, the master equations governing the system dynamics, and the two methods, analytical and numerical, used for calculating the absorption spectrum. In Sec. III we present analytical and numerical results demonstrating the control and tunability of the absorption spectrum. In Sec. IV we present conclusions.

II. MODEL OF THE TWO-LEVEL SYSTEM COUPLED TO THE ELECTROMAGNETIC RADIATION BATH

We model the quantum emitter as a TLS with the ground state $|g\rangle$ and the excited state $|e\rangle$, separated in energy by $E_e - E_g = \hbar\omega_1$; below we set $\hbar = 1$. Initially, at time $t = 0$, the excited state is occupied, and the ground state is empty. The TLS is coupled to a photon bath and is periodically driven by pulses of the laser field with the Rabi frequency Ω. Within the rotating-wave approximation (RWA) [30], in the reference frame rotating at frequency ω_0, the system in

question is described by the Hamiltonian

$$H = \sum_k \omega_k a_k^\dagger a_k + \frac{\Delta}{2}\sigma_z - i\sum_k g_k(a_k^\dagger \sigma_- - a_k \sigma_+)$$
$$+ \frac{\Omega_x(t)}{2}(\sigma_+ + \sigma_-), \tag{1}$$

where $\Delta = \omega_1 - \omega_0$ is the detuning of the TLS's transition frequency from the carrier frequency of the pulses; here we introduced the standard pseudospin Pauli operators for the TLS, namely, $\sigma_z = |e\rangle\langle e| - |g\rangle\langle g|$, $\sigma_+ = |e\rangle\langle g|$, and $\sigma_- = |g\rangle\langle e| = (\sigma_+)^\dagger$. Furthermore, $a_k^\dagger$ and a_k are, respectively, the creation and annihilation operators for a photon of mode k with frequency ω_k, and g_k is the strength of coupling to the TLS. Note that in the rotating frame all frequencies are measured from the pulse carrier frequency ω_0, so that the zero frequency in the rotating frame corresponds to ω_0 in the laboratory frame; we take it as the target frequency for our TLS. The detuning Δ is assumed to be static on the time scale of interest, as is the case for stable emitters, but the value of Δ is not known to an experimentalist because of the slow spectral diffusion, so the goal is to make the absorption spectrum independent of Δ.

The time-dependent driving $\Omega_x(t)$ in Eq. (1) represents the control pulses; here we consider the simple situation of square-shaped pulses, with $\Omega_x(t) = \Omega$ during the pulses and zero otherwise. In fact, below we assume that the pulses are almost instantaneous, i.e., that Ω is much larger than all other relevant energy scales, and that each pulse performs an almost instantaneous 180° rotation of the TLS around the x axis, interchanging $|e\rangle$ and $|g\rangle$; this assumption will be discussed further below. In the absence of control ($\Omega_x(t) \equiv 0$), the system exhibits spontaneous decay, and the corresponding emission rate is $\Gamma = 2\pi \int g_k^2 \, \delta(\omega_k - \Delta) \, dk$; we normalize our energy and time units so that $\Gamma = 2$, and the corresponding spontaneous emission line has a simple Lorentzian shape $1/(1 + \omega^2)$, with the half width equal to 1. In other words, frequencies and times below are measured in units of $\Gamma/2$ and $(\Gamma/2)^{-1}$, respectively.

The absorption spectrum is defined here as the energy absorbed by the TLS during the time interval $0 \leqslant t \leqslant T$ from a weak probing field of frequency ω. The probing field is assumed to be weak enough that it does not significantly affect the population of each state [28,31]; our goal is to calculate the absorption as a function of frequency and time T. Note that the shape of spectra calculated below is established on a time scale of one to two spontaneous emission times, and after that the spectral features increase in amplitude almost linearly with time, so that at longer times T the spectra can be reinterpreted in a standard way via the rate of the energy absorption (absorbed power). In order to be able to describe the absorption (emission) process at earlier times, we calculate the absorbed (emitted) energy, following the standard idealized approach [32]. In general, definition and analysis of the time-dependent spectrum is a nontrivial task [33–35], especially at very short times, where the non-Markovian effects may play a role; that is beyond the scope of our work.

To understand the dynamics of the system, we analyze the time evolution of the density matrix of the emitter, which is

written as

$$\rho(t) = \rho_{ee}(t)|e\rangle\langle e| + \rho_{eg}(t)|e\rangle\langle g|$$
$$+ \rho_{ge}(t)|g\rangle\langle e| + \rho_{gg}(t)|g\rangle\langle g|, \quad (2)$$

with $\rho_{ge}^* = \rho_{eg}$. For the TLS described by the above Hamiltonian (1), within the Markovian approximation, the density-matrix operator is governed by the master equations [30] in the rotating-wave approximation:

$$\dot{\rho}_{ee} = i\frac{\Omega_x(t)}{2}(\rho_{eg} - \rho_{ge}) - \Gamma\rho_{ee},$$

$$\dot{\rho}_{gg} = -i\frac{\Omega_x(t)}{2}(\rho_{eg} - \rho_{ge}) + \Gamma\rho_{ee},$$

$$\dot{\rho}_{ge} = \left(i\Delta - \frac{\Gamma}{2}\right)\rho_{ge} - i\frac{\Omega_x(t)}{2}(\rho_{ee} - \rho_{gg}), \quad (3)$$

$$\dot{\rho}_{eg} = \left(-i\Delta - \frac{\Gamma}{2}\right)\rho_{eg} + i\frac{\Omega_x(t)}{2}(\rho_{ee} - \rho_{gg}).$$

Since the pulse driving is assumed to be strong and short ($\Omega \gg \Delta, \Gamma$), the pulses can be considered instantaneous; our previous studies [23] have shown that even moderate driving strength [of the order of 1 GHz for nitrogen-vacancy (NV) centers] is already satisfactory. Each pulse inverts the populations of the excited and ground states and swaps the values of ρ_{eg} and ρ_{ge}, i.e.,

$$\rho(n\tau + 0) = \sigma_x\rho(n\tau - 0)\sigma_x, \quad (4)$$

where $\rho(n\tau - 0)$ and $\rho(n\tau + 0)$ are the density matrices immediately before and after the pulse, respectively, with n being an integer and τ being the period of the pulse sequence; in other words, the pulses interchange ρ_{ee} with ρ_{gg} and ρ_{eg} with ρ_{ge}.

We want to determine the energy absorbed from a weak probing field by the TLS subjected to the periodic sequence of the π pulses. Since the effect of the probing field is small, the absorption spectrum can be calculated within the linear response theory, so that the absorbed energy $Q(\omega)$ is given by [28,31]

$$Q(\omega) = 2A^2\mathrm{Re}\left\{\int_0^T dt \int_0^{T-t} d\theta \right.$$
$$\left. \times \langle[\sigma_-(t), \sigma_+(t+\theta)]\rangle e^{-i\omega\theta}\right\}, \quad (5)$$

where $[O_1, O_2]$ is the commutator of operators O_1 and O_2 and the angle brackets represent the expectation values evaluated in the absence of the probing field. Here $\sigma_-(t)$ and $\sigma_+(t+\theta)$ are the time-dependent operators in the Heisenberg representation, and the expectation values are taken with respect to the initial state of the two-level system (in our case, fully occupied excited state and empty ground state). The constant A is independent of the pulse parameters and does not affect the spectral shape, determining only the absolute scale of the absorbed energy. Expression (5) can be rewritten as

$$Q(\omega) = 2A^2\mathrm{Re}\{\mathcal{P}_2(\omega) - \mathcal{P}_1(\omega)\}$$
$$= P_2(\omega) - P_1(\omega), \quad (6)$$

where

$$\mathcal{P}_2(\omega) = \int_0^T dt \int_0^{T-t} d\theta \,\langle\sigma_-(t)\sigma_+(t+\theta)\rangle e^{-i\omega\theta} \quad (7)$$

and

$$\mathcal{P}_1(\omega) = \int_0^T dt \int_0^{T-t} d\theta \,\langle\sigma_+(t+\theta)\sigma_-(t)\rangle e^{-i\omega\theta}. \quad (8)$$

The term $P_1(\omega) = 2A^2\mathrm{Re}\{\mathcal{P}_1(\omega)\}$ can be viewed as the direct emission of the two-level system, and $P_2(\omega) = 2A^2\mathrm{Re}\{\mathcal{P}_2(\omega)\}$ can be viewed as the direct absorption, so that the difference yields the net absorption [36]. We evaluate the terms $P_1(\omega)$ and $P_2(\omega)$ separately and obtain the total absorption spectrum $Q(\omega)$ by taking the difference.

To evaluate the emission spectrum, it is convenient to reexpress the two-time correlation function $\langle\sigma_+(t+\theta)\sigma_-(t)\rangle$ as a single-time expectation value [32,36–40], according to

$$\langle\sigma_+(t+\theta)\sigma_-(t)\rangle$$
$$= \mathrm{Tr}[\rho(0)U^{-1}(0, t+\theta)\sigma_+ U(0, t+\theta)U^{-1}(0, t)\sigma_- U(0, t)]$$
$$= \mathrm{Tr}[\sigma_-\rho(t)U^{-1}(t, t+\theta)\sigma_+ U(t, t+\theta)]$$
$$= \mathrm{Tr}[\rho'(t, t+\theta)\sigma_+], \quad (9)$$

where σ_+ and σ_- are the time-independent Pauli operators in the Schrödinger representation and $U(t_1, t_2)$ is the evolution operator of the emitter from time t_1 to time t_2, as determined by the master equation (3). The calculations are simplified by introducing the matrix $\rho'(t, s)$; its initial value at $s = t$ is $\rho'(t, t) = \sigma_-\rho(t)$, and its further evolution from $s = t$ to $s = t + \theta$ is governed by the emitter's evolution operator $U(t, t+\theta)$, so that $\rho'(t, t+\theta) = U(t, t+\theta)\rho'(t, t)U^{-1}(t, t+\theta)$. In this way the evaluation of the two-time correlators becomes rather straightforward (but lengthy; see the Appendix for details), and the function $P_1(\omega)$ can be obtained analytically and/or numerically. In order to calculate the function $P_2(\omega)$, we use the same procedure, simplifying the two-time correlation function as

$$\langle\sigma_-(t)\sigma_+(t+\theta)\rangle = \mathrm{Tr}[\sigma_+\rho''(t, t+\theta)] \quad (10)$$

by introducing the matrix $\rho''(t) = \rho(t)\sigma_-$, whose time evolution is also governed by $U(t, t+\theta)$, i.e., $\rho''(t, t+\theta) = U(t, t+\theta)\rho''(t, t)U^{-1}(t, t+\theta)$. Note that ρ' and ρ'' are not density matrices, and the symmetries of the proper density matrix $\rho(t)$ (such as $\rho_{gg} = 1 - \rho_{ee}$ and/or $\rho_{ge}^* = \rho_{eg}$) are not applicable to ρ' and ρ''.

In the absence of the pulses, the absorption spectrum has a Lorentzian-shaped profile centered at the emitter's frequency that equals the detuning Δ (Fig. 1). In the presence of the pulses, we calculated the absorption spectrum both analytically and numerically by iteratively evolving the density-matrix operator between successive pulses on a discrete time grid, using the equations of motion (3), with the initial conditions $\rho_{ee} = 1$, $\rho_{eg} = \rho_{ge} = \rho_{gg} = 0$, and then making use of (9) and (10) to calculate the two-time correlation functions.

A. Numerical solution

To find the solution numerically, we divide the time axis in intervals of length τ (equal to the interpulse separation), and each interval between the pulses is further discretized into

smaller steps of length Δt. The goal is to find the two-time correlators $\langle \sigma_-(t)\sigma_+(t+\theta) \rangle$ and $\langle \sigma_-(t)\sigma_+(t+\theta) \rangle$ for each value of t and θ on this time grid and use Fourier transform to find $P_1(\omega)$ and $P_2(\omega)$, whose difference gives the absorption spectrum $Q(\omega)$.

We start at $t = 0$ with the known initial conditions for $\rho(t)$ and use Eq. (3) to evolve all elements of the density matrix $\rho(t)$ from time t to $t + \Delta t$, and we repeat this integration up to $t = \tau$. Then the π pulse is applied to the system, transforming the density matrix in accordance with Eq. (4), and the iterative integration is resumed to propagate the density matrix from $t = \tau$ to $t = 2\tau$, until another pulse is applied at 2τ. The process is repeated until time $T = N_p\tau$ is reached, where N_p is the total number of pulses. In this way we can obtain the elements of $\rho'(t,t)$ and $\rho''(t,t)$ for every $t \in [0, N_p\tau]$. Then, for each time t we propagate the matrices ρ' and ρ'' from time t to time $t + \theta$ by solving the master equation (3); the values $\rho'(t,t)$ and $\rho''(t,t)$ serve as initial conditions. As a result, we obtain $\rho'(t,t+\theta)$ and $\rho''(t,t+\theta)$ for all values of $\theta \in [0, T-t]$. This procedure produces the two-time correlators $\langle \sigma_+(t+\theta)\sigma_-(t) \rangle$ and $\langle \sigma_-(t)\sigma_+(t+\theta) \rangle$ [see Eqs. (9) and (10)]. Finally, Fourier transform with respect to θ and integration over t give us $\mathcal{P}_1(\omega)$ and $\mathcal{P}_2(\omega)$, thus determining the absorption spectrum $Q(\omega)$.

B. Analytical solution

The analytical solution for the density-matrix evolution between the pulses can be obtained directly from Eq. (3) and combined with the analytically calculated transformation of the density matrix by pulses as described by Eq. (4), thus providing a fully analytical solution to the problem. The corresponding calculation is quite lengthy and is presented in detail in the Appendix. In the limit of long T (i.e., large number of pulses N_p), the resulting expression for $\mathcal{P}_1(\omega)$ is

$$\mathcal{P}_1(\omega) = \frac{1}{(1+e^{-\Gamma\tau})\gamma_0}\left[\left(\frac{1-e^{-\Gamma\tau}}{\Gamma} - e^{-\gamma_0\tau}\frac{e^{\gamma_2\tau}-1}{\gamma_2}\right.\right.$$
$$+ \frac{e^{\gamma_2\tau}-1}{\gamma_2}\frac{1-e^{-\gamma_0\tau}}{e^{2\gamma_1\tau}-1}\left)\left(N_p + \frac{e^{-\Gamma\tau}}{1+e^{-\Gamma\tau}}\right)\right.$$
$$- \frac{e^{\gamma_2\tau}-1}{\gamma_2}\frac{1-e^{-\gamma_0\tau}}{e^{2\gamma_1\tau}-1}\left(2\frac{e^{-N_p\gamma_1\tau}-1}{e^{-2\gamma_1\tau}-1}\right.$$
$$\left.\left.+ (e^{-\Gamma\tau}-e^{-2\Gamma\tau})\frac{e^{-N_p\gamma_1\tau}}{e^{-2\gamma_1\tau}-e^{-2\Gamma\tau}}\right)\right]. \qquad (11)$$

We have also performed a similar calculation for $\mathcal{P}_2(\omega)$, expressing it as $\mathcal{P}_2(\omega) = \mathcal{P}_3(\omega) - \mathcal{P}_1(\omega)$, and the resulting expression for $\mathcal{P}_3(\omega)$ in the long-time limit is

$$\mathcal{P}_3 = \frac{N_p\tau}{\gamma_0} - \frac{N_p}{\gamma_0^2}(1-e^{-\gamma_0\tau})$$
$$+ \frac{e^{\gamma_0\tau}+e^{-\gamma_0\tau}-2}{\gamma_0^2(e^{2\gamma_1\tau}-1)}\left[N_p - \frac{2}{1-e^{-2\gamma_1\tau}}\right], \qquad (12)$$

where $\gamma_0 = i(\omega - \Delta) + \Gamma/2$, $\gamma_1 = i\omega + \Gamma/2$, and $\gamma_2 = i(\omega - \Delta) - \Gamma/2$.
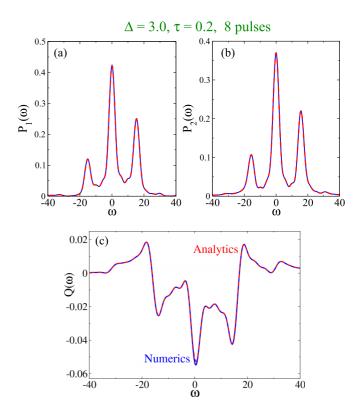

FIG. 2. Absorption spectrum of a two-level system with detuning $\Delta = 3.0$ driven by a periodic sequence of π pulses of period $\tau = 0.2$ after $N_p = 8$ pulses. Panels (a) and (b) show the terms $P_1(\omega)$ (direct emission) and $P_2(\omega)$ (direct absorption), correspondingly, and panel (c) shows the difference between the two terms, which is the total absorption $Q(\omega)$. The results are obtained by solving the master equation numerically (blue solid line) and analytically in the limit of a large number of pulses (red dashed line). The two approaches give very close results despite the assumed limit $N_p \gg 1$ in the analytical result and finite time step used in the Fourier transform of the numerical results.

III. RESULTS

Figure 2 shows the absorption spectrum obtained using both analytical and numerical approaches for a two-level system with $\Delta = 3.0$ and a pulse sequence with $\tau = 0.2$ after $N_p = 8$ pulses. Figures 2(a) and 2(b) show $P_1(\omega)$ and $P_2(\omega)$, respectively, while Fig. 2(c) shows the absorption spectrum obtained by taking their difference according to Eq. (6). In the presence of the pulse control we see the central feature in both spectra $P_1(\omega)$ and $P_2(\omega)$: the peak in the absorption spectrum at the carrier frequency of the pulses ($\omega = 0$ in the rotating frame) and the satellite peaks at the multiples of $\pm\pi/\tau$. These features produce the net absorption spectrum $Q(\omega)$.

Good agreement between numerics and analytics is clearly seen, despite the limit $N_p \gg 1$ used in the analytical result and the numerical Fourier transform of the finite-time-step data in the numerical result. The agreement is further improved by considering the spectrum at longer times (see the Appendix). These results provide clear validation of the tools used in these studies. Moreover, note that the absorption spectrum, as given by Eq. (5), is the difference of two terms of comparable magnitude in a broad frequency range. As a result, it is influenced by numerical errors, but the small discrepancy
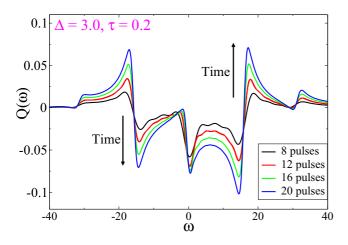
FIG. 3. Absorption spectrum of a two-level system with detuning $\Delta = 3.0$, driven by a periodic sequence of π pulses with period $\tau = 0.2$, after $N_p = 8$ (black), $N_p = 12$ (red), $N_p = 16$ (green), and $N_p = 20$ (blue) pulses. The curves present analytical results; the arrows indicate the increasing number of pulses (increasing total time of the sequence). The overall spectral shape is established early, within one to two spontaneous emission times, and at later times the peaks/dips increase in amplitude.

between the analytical and numerical results shows that this kind of error is not critical. Thus, the numerical solution can be used in future studies of more complex driving protocols, which may not be amenable to an analytical solution.

Figure 3 shows analytical results for the time evolution of the absorption spectrum for $\Delta = 3.0$ and $\tau = 0.2$. The snapshots of the spectrum are presented after $N_p = 8$ (black), $N_p = 12$ (red), $N_p = 16$ (green), and $N_p = 20$ (blue) pulses. The absorption spectra feature a positive part and a negative part. The former corresponds to the "true absorption" [28,41], while the latter corresponds to the stimulated emission, when a photon is absorbed from the driving optical field and another photon is emitted at the probing field frequency. The central dip at $\omega = 0$ corresponds to the stimulated emission at the pulse frequency, and the satellite dips at multiples of $\pm \pi / \tau$, with amplitudes that decrease away from the central frequency. Also, the net absorption peaks are clearly seen on the sides. The overall shape of the spectrum is established early, on a time scale of one to two spontaneous emission times, and later, the amplitude of the peaks/dips just increases with time.

In Fig. 4 we present the dependence of the absorption spectrum for $\Delta = 3.0$ on the period τ of the pulse sequence. The absorption spectrum is shown after eight pulses for $\tau = 0.2$, $\tau = 0.3$, $\tau = 0.4$, and $\tau = 0.5$. The satellites move closer to the central dip, and their relative amplitude increases as τ becomes longer. Also note the increase in the positive fraction of spectral weight with increasing τ.

Finally, we study the dependence of the absorption spectrum on the detuning Δ in order to demonstrate that the pulse protocol stabilizes the positions of different spectral features, making them independent of Δ, and thus suppresses spectral diffusion. The corresponding results are shown in Fig. 5, which presents the spectrum under a pulse sequence of period $\tau = 0.2$ for the detuning values of $\Delta = 3.0$ (black), $\Delta = 4.0$ (red), $\Delta = 5.0$ (green), and $\Delta = 6.0$ (blue) after eight pulses. The
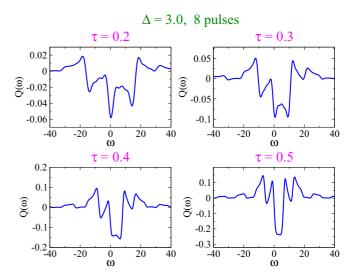

FIG. 4. Absorption spectrum of a two-level system with detuning $\Delta = 3.0$ driven by a periodic sequence of π pulses with the periods $\tau = 0.2$, $\tau = 0.3$, $\tau = 0.4$, and $\tau = 0.5$ after $N_p = 8$ pulses. The curves present analytical results.

shape of the spectrum remains almost the same for all four values of the detuning parameter when τ is kept constant. In fact, we observe that the line shape of the absorption spectrum shows little dependence on Δ as long as $\tau \Delta \lesssim 1$. Figure 5 shows that the fraction of the spectral weight contained in the positive-frequency satellites (with $\omega > \omega_0$) slightly increases with Δ, while the spectral weight of the negative-frequency satellites ($\omega < \omega_0$) correspondingly decreases.

The effect of the control pulses on the spectra can be understood qualitatively by noticing that the shape of the emission/absorption spectra is governed by the rate of the phase accumulation between the ground and excited states of the emitter. Without pulses, in the coordinate frame rotating with the carrier frequency of the driving field ω_0, the phase between the two states accumulates over the time interval T
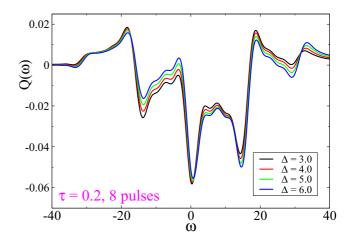

FIG. 5. Absorption spectrum of the TLS with detunings $\Delta = 3.0$ (black), $\Delta = 4.0$ (red), $\Delta = 5.0$ (green), and $\Delta = 6.0$ (blue) driven by a periodic sequence of π pulses of period $\tau = 0.2$ after $N_p = 8$ pulses. The curves present analytical results.

and is equal to $T\Delta$, thus giving rise to a spectral peak at the relative frequency $\omega = \Delta$. But the control pulses periodically invert this phase, preventing its accumulation [23]. As a result, when the phase is inverted sufficiently frequently (small τ), the absorption/emission spectra are controlled primarily by the value of τ and become practically independent of Δ (see the Appendix for theoretical details).

The spectrum created by the control pulses has similarities with the situation of strong continuous driving. The use of short, strong pulses instead of strong continuous driving can minimize some undesirable side effects of strong driving, e.g., ionization of a NV center or a quantum dot by the strong driving field, excitation of the emitter to other (nonresonant) levels, possible ionization of other photosensitive entities in the sample, increased background photon count due to coherent scattering of the driving laser light, etc. Even if the side effects cannot be suppressed completely, the use of the pulses instead of continuous driving restricts these effects to the narrow time windows in the immediate vicinity of the pulses, which could make it easier to detect and control them. Moreover, control of the pulse period gives experimentalists an alternative way to change the system's evolution, which can facilitate engineering of the emission/absorption spectra.

IV. CONCLUSIONS

We have studied the absorption spectrum of a two-level system driven by a periodic sequence of the π pulses. This absorption spectrum is determined by the energy absorbed by the emitter from a probing field weak enough to not significantly affect the population of the excited and ground states. We have solved the problem by integrating the master equation analytically and numerically and obtained from both methods results that are in excellent agreement. The absorption spectrum has a pronounced dip at the pulse carrier frequency (which corresponds to stimulated emission), the net absorption peaks on the sides, and the satellite peaks/dips at multiples of $\pm\pi/\tau$; the spectral weights of the satellites are suppressed away from the central peak. Our results show that for reasonably small τ (say, smaller than half of the spontaneous emission time, $\Gamma\tau < 1/2$) and for moderate detunings, $\Delta\tau \lesssim 1$, the absorption spectrum has a shape with little dependence on Δ, so that all features (stimulated emission dips and the net absorption peaks) are stabilized by the control pulses.

By using the optical control considered in this work (with, possibly, more complex pulse protocols), it is possible to create pairs of quantum nodes, with one node working as an emitter and the other as an absorber, with precisely matching frequencies, and therefore greatly increased entanglement efficiency. In a similar manner, one can use it to improve the coupling of the emitters and absorbers to optical cavities, using the laser pulses to tune both the emission and the absorption lines of the respective quantum nodes, bringing them in resonance with the respective cavities and stabilizing both the emission and absorption features at the desired location.

ACKNOWLEDGMENTS

APPENDIX

Here we present the details of the analytical calculation of the absorption spectrum for a two-level system subjected to a periodic sequence of control pulses. As shown in Refs. [28,41], the absorption spectrum can be determined from the two-time correlation functions of the TLS:

$$Q(\omega) = 2A^2 \times \text{Re}\left\{ \int_0^T dt \int_0^{T-t} d\theta \right.$$
$$\left. \times \langle [\sigma_-(t), \sigma_+(t+\theta)] \rangle e^{-i\omega\theta} \right\}, \quad \text{(A1)}$$

where $[\,,]$ is the commutator of the two enclosed operators and the angle brackets represent the expectation values evaluated in the absence of the probing field. A is a proportionality constant. This can be rewritten as

$$Q(\omega) = 2A^2 \text{Re}\{\mathcal{P}_2(\omega) - \mathcal{P}_1(\omega)\}$$
$$= P_2(\omega) - P_1(\omega), \quad \text{(A2)}$$

with

$$\mathcal{P}_2(\omega) = \int_0^T dt \int_0^{T-t} d\theta \langle \sigma_-(t)\sigma_+(t+\theta)\rangle e^{-i\omega\theta} \quad \text{(A3)}$$

and

$$\mathcal{P}_1(\omega) = \int_0^T dt \int_0^{T-t} d\theta \langle \sigma_+(t+\theta)\sigma_-(t)\rangle e^{-i\omega\theta}. \quad \text{(A4)}$$

The terms $P_1(\omega) = 2A^2 \text{Re}\{\mathcal{P}_1(\omega)\}$ and $P_2(\omega) = 2A^2 \text{Re}\{\mathcal{P}_2(\omega)\}$ can be evaluated separately, and the absorption spectrum can be obtained by taking the difference. To find $\mathcal{P}_2(\omega)$, we express the correlation function as

$$\langle \sigma_-(t)\sigma_+(t+\theta)\rangle$$
$$= \text{Tr}[\rho(0)U^{-1}(0,t)\sigma_- U(0,t)U^{-1}(0,t+\theta)$$
$$\times \sigma_+ U(0,t+\theta)]$$
$$= \text{Tr}[\sigma_+ U(t,t+\theta)U(0,t)\rho(0)U^{-1}(0,t)$$
$$\times \sigma_- U(0,t)U^{-1}(0,t)U^\dagger(t,t+\theta)]$$
$$= \text{Tr}[\sigma_+ U(t,t+\theta)\rho(t)\sigma_- U^{-1}(t,t+\theta)]$$
$$= \text{Tr}[\sigma_+ U(t,t+\theta)\rho''(t,t)U^{-1}(t,t+\theta)]$$
$$= \text{Tr}[\sigma_+\rho''(t,t+\theta)], \quad \text{(A5)}$$

where σ_+ and σ_- are the Pauli operators and $U(t_1,t_2)$ is the operator of the emitter's evolution from t_1 to t_2, as determined by the master equation (3). The subsequent calculations are facilitated by introducing the matrix $\rho''(t,s)$; its initial value at $s = t$ is defined as $\rho''(t,t) = \rho(t)\sigma_-$, and its further evolution from $s = t$ to $s = t + \theta$ is governed by the emitter's evolution operator $U(t,t+\theta)$, so that $\rho''(t,t+\theta) = U(t,t+\theta)\rho''(t,t)U^{-1}(t,t+\theta)$.

It is informative to write $\rho''(t,s)$ explicitly as

$$\rho''(t,s) = \begin{pmatrix} \rho''_{ee}(t,s) & \rho''_{eg}(t,s) \\ \rho''_{ge}(t,s) & \rho''_{gg}(t,s) \end{pmatrix}, \tag{A6}$$

so that

$$\sigma_+\rho''(t+\theta) = \begin{pmatrix} \rho''_{ge}(t,t+\theta) & \rho''_{gg}(t,t+\theta) \\ 0 & 0 \end{pmatrix}, \tag{A7}$$

and the corresponding two-time correlation function is obtained directly as

$$\langle\sigma_-(t)\sigma_+(t+\theta)\rangle = \mathrm{Tr}[\sigma_+\rho''(t,t+\theta)]$$
$$= \rho''_{ge}(t,t+\theta). \tag{A8}$$

The initial condition for ρ'', corresponding to $s = t$, has the form

$$\rho''(t,t) = \rho(t)\sigma_- = \begin{pmatrix} \rho_{eg}(t) & 0 \\ \rho_{gg}(t) & 0 \end{pmatrix}, \tag{A9}$$

which is determined by the elements of the "true" density matrix $\rho_{eg}(t) = \langle e|\rho(t)|g\rangle$ and $\rho_{gg}(t) = \langle g|\rho(t)|g\rangle$ [see Eq. (2)]. Similarly, for $\rho'(t,s)$ the initial conditions at $s = t$ are

$$\rho'_{ee}(t,t) = \rho'_{eg}(t,t) = 0,$$
$$\rho'_{gg}(t,t) = \rho_{eg}(t), \quad \rho'_{ge}(t,t) = \rho_{ee}(t), \tag{A10}$$

and the corresponding two-time correlator is

$$\langle\sigma_+(t+\theta)\sigma_-(t)\rangle = \mathrm{Tr}[\rho'(t,t+\theta)\sigma_+] = \rho'_{ge}(t,t+\theta). \tag{A11}$$

Therefore, our task is reduced to determining $\rho''_{ge}(t,t+\theta)$ and $\rho'_{ge}(t,t+\theta)$.

The master equations characterizing the time evolution of the TLS density matrix are given by Eqs. (3) and (4); the time development of the matrices $\rho''(t,s)$ and $\rho'(t,s)$ also obeys these equations of motion as s increases from t to $t+\theta$. Specifically, when s corresponds to the time interval between the pulses, we have

$$\frac{d}{ds}\rho''_{ee}(t,s) = -\Gamma\,\rho''_{ee}(t,s), \tag{A12}$$

$$\frac{d}{ds}\rho''_{gg}(t,s) = \Gamma\,\rho''_{ee}(t,s), \tag{A13}$$

$$\frac{d}{ds}\rho''_{ge}(t,s) = \left(i\Delta - \frac{\Gamma}{2}\right)\rho''_{ge}(t,s), \tag{A14}$$

$$\frac{d}{ds}\rho''_{eg}(t,s) = \left(-i\Delta - \frac{\Gamma}{2}\right)\rho''_{eg}(t,s) \tag{A15}$$

for any value of the parameter t; the same equations govern the dynamics of ρ'. The effect of the pulses on ρ'' and ρ' is also easily derived from Eq. (4): when $t+s$ coincides with the time of the pulse application, i.e., when $s = n\tau$ for some integer n, the matrix transforms as

$$\rho''(t,n\tau + 0) = \sigma_x\rho''(t,n\tau - 0)\sigma_x, \tag{A16}$$

where $\rho''(t,n\tau - 0)$ and $\rho''(t,n\tau + 0)$ are the matrices immediately before and after the pulse, respectively; in other words, each pulse interchanges ρ''_{ee} with ρ''_{gg} and ρ''_{eg} with ρ''_{ge}; the transformation of ρ' is the same.
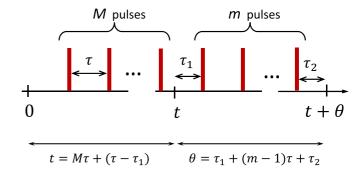

FIG. 6. Schematic of the mutual positions of the time instants t and $t+\theta$ with respect to the pulses.

Let us start with establishing the initial condition for $\rho''(t,s)$ at $s = t$, which is determined by $\rho_{gg}(t)$ and $\rho_{eg}(t)$ [see Eq. (A9)]. First, we note that $\rho_{eg}(t) \equiv 0$. Indeed, the initial conditions at $t = 0$ for the density matrix ρ are

$$\rho_{ee}(0) = 1, \quad \rho_{gg}(0) = \rho_{ge}(0) = \rho_{eg}(0) = 0. \tag{A17}$$

As the master equation (3) show, both quantities ρ_{eg} and ρ_{ge} remain zero before the first pulse [when $\Omega_x(t) \equiv 0$]. The effect of the pulse is to interchange these two values; that is, they both remain zero after the pulse. The same considerations can be applied for the second pulse, third pulse, etc., showing that $\rho_{eg}(t) = \rho_{ge}(t) = 0$ for all t. Thus, to determine $\rho''(t,t)$ we only need to find $\rho_{gg}(t)$. We assume that the time instant t is between the Mth and the $(M+1)$th pulses, i.e., $t = M\tau + (\tau - \tau_1)$ for some $\tau_1 \in [0,\tau]$, as shown in Fig. 6. Immediately before the first pulse, at the time moment $\tau - 0$, we have

$$\rho_{ee}(\tau) = e^{-\Gamma\tau},$$
$$\rho_{gg}(\tau) = 1 - e^{-\Gamma\tau}. \tag{A18}$$

Then at time $2\tau - 0$ we have

$$\rho_{ee}(2\tau) = (1 - e^{-\Gamma\tau})e^{-\Gamma\tau}$$
$$\rho_{gg}(2\tau) = 1 - e^{-\Gamma\tau} + e^{-2\Gamma\tau}, \tag{A19}$$

and at time $3\tau - 0$ we have

$$\rho_{ee}(3\tau) = e^{-\Gamma\tau} - e^{-2\Gamma\tau} + e^{-3\Gamma\tau}$$
$$\rho_{gg}(3\tau) = 1 - e^{-\Gamma\tau} + e^{-2\Gamma\tau} - e^{-3\Gamma\tau}, \tag{A20}$$

$$\vdots$$

so that eventually, right before the Mth pulse, at time $M\tau - 0$

$$\rho_{ee}(M\tau - 0) = \sum_{k=1}^{M}(-1)^{k-1}e^{-k\Gamma\tau} = -\sum_{k=1}^{M}(-1)^{k}e^{-k\Gamma\tau}, \tag{A21}$$

and right after the Mth pulse, which interchanges ρ_{ee} and ρ_{gg},

$$\rho_{ee}(M\tau + 0) = 1 - \rho_{ee}(M\tau - 0) = 1 + \sum_{k=1}^{M}(-1)^{k}e^{-k\Gamma\tau}. \tag{A22}$$

Thus, at the time instant $t = M\tau + (\tau - \tau_1)$, we have

$$\rho_{ee}(t) = \left(1 + \sum_{k=1}^{M}(-1)^k e^{-k\Gamma\tau}\right)e^{-\Gamma(\tau-\tau_1)}$$

$$= \left(\sum_{k=0}^{M}(-1)^k e^{-k\Gamma\tau}\right)e^{-\Gamma(\tau-\tau_1)}$$

$$= \frac{1 - (-1)^{M+1}e^{-(M+1)\Gamma\tau}}{1 + e^{-\Gamma\tau}}e^{-\Gamma(\tau-\tau_1)}, \quad (A23)$$

and since $\rho_{gg}(t) = 1 - \rho_{ee}(t)$, we obtain

$$\rho_{gg}(t) = 1 - \frac{1 - (-1)^{M+1}e^{-(M+1)\Gamma\tau}}{1 + e^{-\Gamma\tau}}e^{-\Gamma(\tau-\tau_1)}. \quad (A24)$$

Having established the explicit initial value of $\rho''(t,t)$, now we can proceed with evaluating the value of $\rho''_{ge}(t,t+\theta)$. Between the pulses both ρ''_{ge} and ρ''_{eg} evolve according to Eqs. (A14) and (A15).

Thus, if t and $t + \theta$ belong to the same interpulse interval (i.e., when $M\tau < t + \theta < (M+1)\tau$), we have

$$\rho''_{ge}(t,t+\theta) = e^{(i\Delta-\frac{\Gamma}{2})\theta}\rho_{gg}(t), \qquad \rho''_{eg} = 0. \quad (A25)$$

With increasing θ, at some point it will become equal to τ_1, and then the instant $t + \theta$ will coincide with the instant when a pulse is applied: $t + \theta = (M+1)\tau + 0$. At this point the time instants t and $t + \theta$ will become separated by one pulse, and the value of ρ''_{ge} will be interchanged with ρ''_{eg}; that is, when $\theta = \tau_1 + 0$, we will have already

$$\begin{aligned} \rho''_{ge}(t,t+\theta) &= 0, \\ \rho''_{eg}(t,t+\theta) &= e^{(i\Delta-\frac{\Gamma}{2})\tau_1}\rho_{gg}(t). \end{aligned} \quad (A26)$$

At this point, the accumulation rate of the phase in ρ''_{ge} and ρ''_{eg} changes sign: note that the factors on the right-hand sides of Eqs. (A14) and (A15) have opposite imaginary parts, $i\Delta$ and $-i\Delta$, respectively. Thus, right before the next pulse, when $t + \theta = (M+2)\tau - 0$ (i.e., when $\theta = \tau + \tau_1 - 0$), we will have

$$\begin{aligned} \rho''_{ge}(t,t+\theta) &= 0, \\ \rho''_{eg}(t,t+\theta) &= e^{(i\Delta-\frac{\Gamma}{2})\tau_1}e^{(-i\Delta-\frac{\Gamma}{2})\tau}\rho_{gg}(t), \end{aligned} \quad (A27)$$

and right after the pulse, when $t + \theta = (M+2)\tau + 0$ (i.e., when $\theta = \tau + \tau_1 + 0$), the values will be interchanged again:

$$\begin{aligned} \rho''_{ge}(t,t+\theta) &= e^{(i\Delta-\frac{\Gamma}{2})\tau_1}e^{(-i\Delta-\frac{\Gamma}{2})\tau}\rho_{gg}(t), \\ \rho''_{eg}(t,t+\theta) &= 0. \end{aligned} \quad (A28)$$

Proceeding further in this way, right before the next pulse, at $\theta = \tau_1 + 2\tau - 0$, we get

$$\begin{aligned} \rho''_{ge}(t,t+\theta) &= e^{(i\Delta-\frac{\Gamma}{2})\tau_1}e^{-\Gamma\tau}\rho_{gg}(t), \\ \rho''_{eg}(t,t+\theta) &= 0. \end{aligned} \quad (A29)$$

Note that the phase of ρ''_{ge} still equals to $i\Delta\tau_1$ because after each pulse the phase accumulation rate changes sign. Further, at $\theta = \tau_1 + 3\tau - 0$,

$$\begin{aligned} \rho''_{ge}(t,t+\theta) &= 0, \\ \rho''_{eg}(t,t+\theta) &= e^{(i\Delta-\frac{\Gamma}{2})\tau_1-i\Delta\tau-\frac{3\Gamma}{2}\tau}\rho_{gg}(t). \end{aligned} \quad (A30)$$

Thus, we obtain that for $\theta = \tau_1 + (m-1)\tau - 0$ with even m, as shown in Fig. 6,

$$\begin{aligned} \rho''_{ge}(t,t+\theta) &= 0, \\ \rho''_{eg}(t,t+\theta) &= e^{(i\Delta-\frac{\Gamma}{2})\tau_1-i\Delta\tau-\frac{(m-1)\Gamma}{2}\tau}\rho_{gg}(t), \end{aligned} \quad (A31)$$

and for $\theta = \tau_1 + (m-1)\tau + \tau_2$ with even m and $\tau_2 < \tau$,

$$\begin{aligned} \rho''_{ge}(t,t+\theta) &= e^{(i\Delta-\frac{\Gamma}{2})\tau_1-i\Delta\tau-\frac{(m-1)\Gamma}{2}\tau}e^{i\Delta\tau_2-\frac{\Gamma}{2}\tau_2}\rho_{gg}(t) \\ &= e^{-\Gamma\theta/2}e^{i\Delta(\tau_1+\tau_2-\tau)}\rho_{gg}(t), \\ \rho''_{eg}(t,t+\theta) &= 0. \end{aligned} \quad (A32)$$

Altogether, we can write

$$\rho''_{ge}(t,t+\theta) = f(t,\theta)\rho_{gg}(t), \quad (A33)$$

with $\rho_{gg}(t)$ given above by Eq. (A24), and
(i) for t and $t + \theta$ in the same pulse interval,

$$f(t,\theta) = e^{(i\Delta-\frac{\Gamma}{2})\theta}, \quad (A34)$$

(ii) for t and $t + \theta$ separated by an odd number of pulses,

$$f(t,\theta) = 0, \quad (A35)$$

(iii) for t and $t + \theta$ separated by an even number m of pulses, i.e., when $\theta = \tau_1 + (m-1)\tau + \tau_2$ with even m and $\tau_2 < \tau$ (Fig. 6),

$$f(t,\theta) = e^{-\Gamma\theta/2}e^{i\Delta(\tau_1+\tau_2-\tau)} = e^{-\Gamma\theta/2}e^{i\Delta(\theta-m\tau)}. \quad (A36)$$

Note that, due to the pulses, the phase of the function $f(t,\theta)$ does not grow linearly with θ, being confined to the interval $[-\tau\Delta,\tau\Delta]$ at all values of t and θ. This is the reason why, for small interpulse delay $\tau \ll \Delta^{-1}$, both emission and absorption are concentrated in the vicinity of $\omega = 0$ instead of $\omega = \Delta$.

With this result, we can now rewrite the direct absorption integral $\mathcal{P}_2(\omega)$ in the form

$$\mathcal{P}_2(\omega) = \int_0^T dt\, \rho_{gg}(t)\int_0^{T-t} d\theta f(t,\theta)e^{-i\omega\theta}. \quad (A37)$$

First, let us evaluate the inner integral, which we will denote as I_θ, using the explicit form of $f(t,\theta)$ above:

$$\begin{aligned} I_\theta &= \int_0^{\tau_1} d\theta\, e^{-i\omega\theta}e^{(i\Delta-\Gamma/2)\theta} \\ &+ \int_{\tau_1+\tau}^{\tau_1+2\tau} d\theta\, e^{-i\omega\theta}e^{-i2\Delta\tau+(i\Delta-\Gamma/2)\theta} \\ &+ \int_{\tau_1+3\tau}^{\tau_1+4\tau} d\theta\, e^{-i\omega\theta}e^{-i4\Delta\tau+(i\Delta-\Gamma/2)\theta} + \cdots \\ &+ \int_{\substack{\tau_1+(m-1)\tau \\ \text{even } m}}^{\tau_1+m\tau} d\theta\, e^{-i\omega\theta}e^{-im\Delta\tau+(i\Delta-\Gamma/2)\theta} + \cdots \\ &= \frac{e^{[i(\Delta-\omega)-\Gamma/2]\tau_1}-1}{i(\Delta-\omega)-\Gamma/2} \\ &+ \sum_{\substack{m=2 \\ \text{even } m}}^{m_{\max}}\int_{\tau_1+(m-1)\tau}^{\tau_1+m\tau} d\theta\, e^{-i\omega\theta}e^{[-im\Delta\tau+(i\Delta-\Gamma/2)\theta]}, \quad (A38) \end{aligned}$$

where the summation is over even values of m and $m_{\max}$ is the maximum value of m; since it has to be even, its specific value

depends on whether M is odd or even (see below for details). Defining $\gamma_0 = i(\omega - \Delta) + \Gamma/2$, we can write

$$
\begin{aligned}
I_\theta &= \frac{1 - e^{-\gamma_0 \tau_1}}{\gamma_0} + \sum_{\substack{m=2 \\ \text{even } m}}^{m_{\max}} e^{-im\Delta\tau} \frac{e^{-\gamma_0(\tau_1+(m-1)\tau)} - e^{-\gamma_0(\tau_1+m\tau)}}{\gamma_0} \\
&= \frac{1 - e^{-\gamma_0 \tau_1}}{\gamma_0} + \frac{e^{-\gamma_0 \tau_1}}{\gamma_0}(e^{\gamma_0\tau} - 1)\frac{1 - e^{-m_{\max}\gamma_1\tau}}{e^{2\gamma_1\tau} - 1}, \quad \text{(A39)}
\end{aligned}
$$

where we have introduced $\gamma_1 = \Gamma/2 + i\omega$. Note that this result correctly reproduces the situation of $m_{\max} < 2$, i.e., when $m_{\max} = 0$; this happens when t belongs to the last interpulse interval of the sequence and θ varies only from zero to τ_1. Then the value of I_θ is given by the first integral in Eq. (A38), while the remaining sum over m is zero. Thus, we do not need to worry about this special case in the calculations below.

Now we need to evaluate the outer integral:

$$
\mathcal{P}_2(\omega) = \int_0^T dt \, \rho_{gg}(t) I_\theta, \quad \text{(A40)}
$$

with the quantity ρ_{gg} calculated earlier,

$$
\begin{aligned}
\rho_{gg}(t) &= 1 - \rho_0(M)e^{-\Gamma(\tau-\tau_1)} \\
&= 1 - \frac{1 - (-1)^{M+1}e^{-(M+1)\Gamma\tau}}{1 + e^{-\Gamma\tau}}e^{-\Gamma(\tau-\tau_1)}, \quad \text{(A41)}
\end{aligned}
$$

where we introduced the shorthand notation $\rho_0(M)$ for the awkward fraction appearing on the second line. In this way, we represent $\mathcal{P}_2$ as

$$
\begin{aligned}
\mathcal{P}_2 &= \int_0^T dt \, I_\theta - \int_0^\tau dt \, \rho_0(0)e^{-\Gamma(\tau-\tau_1)} I_\theta \quad \text{(A42)} \\
&\quad - \int_\tau^{2\tau} dt \, \rho_0(1)e^{-\Gamma(\tau-\tau_1)} I_\theta \\
&\quad - \cdots - \int_{(N_p-1)\tau}^{N_p\tau} dt \, \rho_0(N_p-1)e^{-\Gamma(\tau-\tau_1)} I_\theta \quad \text{(A43)} \\
&= \int_0^T dt \, I_\theta \\
&\quad - \sum_{M=0}^{N_p-1} \rho_0(M)\int_0^\tau dt_1 \, e^{-\Gamma t_1}\left(\frac{1}{\gamma_0} + e^{-\gamma_0\tau_1}I_\theta^{(1)}\right), \\
&\qquad\qquad\qquad\qquad\qquad\qquad\qquad\qquad \text{(A44)}
\end{aligned}
$$

where we have defined $t_1 = t - M\tau = \tau - \tau_1$ and

$$
\begin{aligned}
I_\theta &= \frac{1}{\gamma_0} + e^{-\gamma_0\tau_1}I_\theta^{(1)}, \\
I_\theta^{(1)} &= -\frac{1}{\gamma_0} + \frac{e^{\gamma_0\tau} - 1}{\gamma_0}\frac{1 - e^{-m_{\max}\gamma_1\tau}}{e^{2\gamma_1\tau} - 1} \\
&= -1/\gamma_0 + I_\theta^{(2)}, \quad \text{(A45)}
\end{aligned}
$$

where we introduced the shorthand notation $I_\theta^{(2)}$ for another awkward fraction, the second summand on the second line above.

Now we have

$$
\begin{aligned}
\mathcal{P}_2 &= -\sum_{M=0}^{N_p-1} \rho_0(M)\int_0^\tau dt_1 \, e^{-\Gamma t_1}\left(\frac{1}{\gamma_0} + e^{-\gamma_0(\tau-t_1)}I_\theta^{(1)}\right) \\
&\quad + \int_0^T dt \, I_\theta \\
&= -\sum_{M=0}^{N_p-1} \rho_0(M)\left[\frac{1 - e^{-\Gamma\tau}}{\gamma_0\Gamma} + I_\theta^{(1)}e^{-\gamma_0\tau}\frac{e^{\gamma_2\tau} - 1}{\gamma_2}\right] \\
&\quad + \mathcal{P}_3, \quad \text{(A46)}
\end{aligned}
$$

with $\mathcal{P}_3 = \int_0^T dt \, I_\theta$ and $\gamma_2 = \gamma_0 - \Gamma = i(\omega - \Delta) - \frac{\Gamma}{2}$.

Below we will show that the first sum gives exactly the contribution from the stimulated emission $\mathcal{P}_1(\omega)$. It is convenient to calculate the simpler term $\mathcal{P}_3$ first. We can rewrite $\mathcal{P}_3$ as

$$
\begin{aligned}
\mathcal{P}_3 &= \int_0^T \frac{dt}{\gamma_0} + \int_0^\tau dt \, e^{-\gamma_0\tau_1}I_\theta^{(1)} \\
&\quad + \cdots + \int_{(N_p-1)\tau}^{N_p\tau} dt \, e^{-\gamma_0\tau_1}I_\theta^{(1)} \\
&= \frac{N_p\tau}{\gamma_0} + e^{-\gamma_0\tau}\sum_{M=0}^{N_p-1} I_\theta^{(1)}\int_0^\tau dt_1 \, e^{\gamma_0 t_1} \\
&= \frac{N_p\tau}{\gamma_0} + \sum_{M=0}^{N_p-1} I_\theta^{(1)}\frac{1 - e^{-\gamma_0\tau}}{\gamma_0}. \quad \text{(A47)}
\end{aligned}
$$

With the explicit form of $I_\theta^{(1)}$ given above, we have

$$
\begin{aligned}
\mathcal{P}_3 &= \frac{N_p\tau}{\gamma_0} - \sum_{M=0}^{N_p-1}\frac{1 - e^{-\gamma_0\tau}}{\gamma_0^2} + \sum_{M=0}^{N_p-1}\frac{1 - e^{-\gamma_0\tau}}{\gamma_0^2}I_\theta^{(2)} \\
&= \frac{N_p\tau}{\gamma_0} - \frac{N_p}{\gamma_0^2}(1 - e^{-\gamma_0\tau}) + \mathcal{P}_4, \quad \text{(A48)}
\end{aligned}
$$

where

$$
\begin{aligned}
\mathcal{P}_4 &= \frac{1 - e^{-\gamma_0\tau}}{\gamma_0}\frac{e^{\gamma_0\tau} - 1}{\gamma_0}\sum_{M=0}^{N_p-1}\frac{1 - e^{-\gamma_1\tau m_{\max}}}{e^{2\gamma_1\tau} - 1} \\
&= \frac{e^{\gamma_0\tau} + e^{-\gamma_0\tau} - 2}{\gamma_0^2(e^{2\gamma_1\tau} - 1)}\left[N_p - \sum_{M=0}^{N_p-1} e^{-\gamma_1\tau m_{\max}}\right]. \\
&\qquad\qquad\qquad\qquad\qquad\qquad\qquad\qquad \text{(A49)}
\end{aligned}
$$

In order to calculate the last sum in the equation above, we need to determine $m_{\max}$. To do this let us consider the case of $N_p = 2K$, i.e., when the number K of the full cycles of the sequence has been applied to the TLS. Let us recall that we represent $t = M\tau + (\tau - \tau_1)$; that is, M is the number of pulses between zero and t. The number of pulses separating t and $t + \theta$ is m, and the maximum value of θ is $\theta_{\max} = T - t$, which limits the maximum value of m; however, $f(t,\theta)$ is zero if m is odd, so that $m_{\max}$ should be even. Therefore, starting from larger values of t, we obtain the following:

(i) If $t \in [T - \tau, T]$, then $\theta_{\max} = (T - t) \in [0, \tau]$, so that if $M = 2K - 1$, then $m_{\max} = 0$.

(ii) If $t \in [T - 2\tau, T - \tau]$, then $\theta_{\max} = (T - t) \in [\tau, 2\tau]$, so that if $M = 2K - 2$, then $m_{\max} = 0$ because $m_{\max}$ should be even.

(iii) If $t \in [T - 3\tau, T - 2\tau]$, then $\theta_{\max} = (T - t) \in [2\tau, 3\tau]$, so that if $M = 2K - 3$, then $m_{\max} = 2$.

(iv) If $t \in [T - 4\tau, T - 3\tau]$, then $\theta_{\max} = (T - t) \in [3\tau, 4\tau]$, so that if $M = 2K - 4$, then $m_{\max} = 2$ (should be even).

(v) If $t \in [T - 5\tau, T - 4\tau]$, then $\theta_{\max} = (T - t) \in [4\tau, 5\tau]$, so that if $M = 2K - 5$, then $m_{\max} = 4$.

(vi) If $t \in [T - 6\tau, T - 5\tau]$, then $\theta_{\max} = (T - t) \in [5\tau, 6\tau]$, so that if $M = 2K - 6$, then $m_{\max} = 4$ (should be even).

(vii) etc.

(viii) If $t \in [\tau, 2\tau]$, then $\theta_{\max} = (T - t) \in [T - 2\tau, T - \tau]$, so that if $M = 1$, then $m_{\max} = 2K - 2$.

(ix) If $t \in [0, \tau]$, then $\theta_{\max} = (T - t) \in [T - \tau, T]$, so that if $M = 0$, then $m_{\max} = 2K - 2$ (should be even).

To summarize, if we parametrize $M = 2n$ for even M and $M = 2n + 1$ for odd M, where n varies from 0 to $K - 1$, then $m_{\max} = 2(K - n - 1)$ for both $M = 2n$ and $M = 2n + 1$.

Thus, the last sum in Eq. (A49) is calculated as

$$\sum_{M=0}^{N_p-1} e^{-\gamma_1 \tau m_{\max}} = 2 \sum_{n=0}^{K-1} e^{-2\gamma_1 \tau (K-n-1)}$$

$$= 2 \frac{1 - e^{-\gamma_1 \tau N_p}}{1 - e^{-2\gamma_1 \tau}}, \tag{A50}$$

where the factor 2 appears because $m_{\max}$ is the same for both $M = 2n$ and $M = 2n + 1$, so that the sums over odd M and even M are combined. Putting all terms together, we obtain
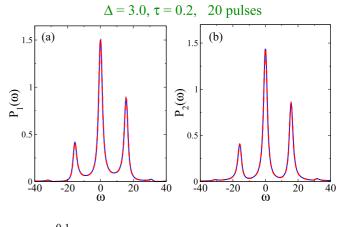
$$\mathcal{P}_3 = \frac{N_p \tau}{\gamma_0} - \frac{N_p}{\gamma_0^2}(1 - e^{-\gamma_0 \tau}) + \frac{e^{\gamma_0 \tau} + e^{-\gamma_0 \tau} - 2}{\gamma_0^2(e^{2\gamma_1 \tau} - 1)}$$

$$\times \left[N_p - 2 \frac{1 - e^{-\gamma_1 \tau N_p}}{1 - e^{-2\gamma_1 \tau}} \right]. \tag{A51}$$

Now, the calculation of the emission term $\mathcal{P}_1$ can be simplified if we notice that $\rho'(t, s)$ obeys the same equations of motion as $\rho''(t, s)$ and is transformed by the pulses in exactly the same way. Therefore, the quantity $\rho'_{ge}(t, s)$ (which determines $\mathcal{P}_1$) evolves in exactly the same way as $\rho''_{ge}(t, s)$, and the difference between them is only in the initial condition: at $s = t$ we have $\rho'_{ge}(t, t) = \rho_{ee}(t)$, while $\rho''_{ge}(t, t) = \rho_{gg}(t) = 1 - \rho_{ee}(t)$. Thus, the reasoning that was used in deriving Eqs. (A25)–(A32) can be directly applied to $\rho'_{ge}(t, s)$ if $\rho_{gg}(t)$ is substituted by $\rho_{ee}(t)$ due to the linearity of the master equations. As a result, we immediately see that $\rho'_{ge}(t, t + \theta)$ has the form

$$\rho'_{ge}(t, t + \theta) = f(t, \theta)\rho_{ee}(t) \tag{A52}$$

with the same function $f(t, \theta)$. Thus, the integral I_θ can be used without modifications in the calculation of $\mathcal{P}_1$, and since $\rho_{gg}(t) = 1 - \rho_{ee}(t)$, we immediately obtain

$$\mathcal{P}_1(\omega) = \int_0^T \rho_{ee}(t) I_\theta \, dt = \int_0^T [1 - \rho_{gg}(t)] I_\theta \, dt = \mathcal{P}_3 - \mathcal{P}_2. \tag{A53}$$
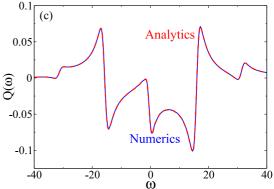

FIG. 7. Absorption spectrum of a two-level system with detuning $\Delta = 3.0$ driven by a periodic sequence of π pulses of period $\tau = 0.2$ after 20 pulses. The results are obtained by solving the master equation numerically (blue solid line) or analytically in the limit of a large number of pulses (red dashed line). We see that indeed the agreement between the numerical and analytical results is better at longer times (for a large number of pulses).

Comparing this expression with Eq. (A46) above, we obtain an explicit expression,

$$\mathcal{P}_1 = \sum_{M=0}^{N_p-1} \rho_0(M) \int_0^\tau dt_1 \, e^{-\Gamma t_1} \left(\frac{1}{\gamma_0} + e^{-\gamma_0(\tau - t_1)} I_\theta^{(1)} \right)$$

$$= \sum_{M=0}^{N_p-1} \rho_0(M) \left[\frac{1 - e^{-\Gamma \tau}}{\gamma_0 \Gamma} + I_\theta^{(1)} e^{-\gamma_0 \tau} \frac{e^{\gamma_2 \tau} - 1}{\gamma_2} \right]. \tag{A54}$$

Now let us evaluate the sums appearing in this expression. First, we need the sum

$$\sum_{M=0}^{N_p-1} \rho_0(M) = \frac{1}{1 + e^{-\Gamma \tau}} \sum_{M=0}^{N_p-1} [1 + e^{-\Gamma \tau}(-e^{-\Gamma \tau})^M]$$

$$= \frac{N_p}{1 + e^{-\Gamma \tau}} + \frac{e^{-\Gamma \tau}}{1 + e^{-\Gamma \tau}} \frac{1 - (-e^{-\Gamma \tau})^{N_p}}{1 + e^{-\Gamma \tau}}, \tag{A55}$$

and for sufficiently large N_p, when the exponentially small terms can be omitted, this yields

$$\sum_{M=0}^{N_p-1} \rho_0(M) \approx \frac{N_p}{1+e^{-\Gamma\tau}} + \frac{e^{-\Gamma\tau}}{(1+e^{-\Gamma\tau})^2}. \qquad (A56)$$

The second required sum is

$$\sum_{M=0}^{N_p-1} \rho_0(M) e^{-\gamma_1\tau m_{\max}}, \qquad (A57)$$

and in order to evaluate it we use the same parametrization as above, $M = 2n$ for even M and $M = 2n+1$ for odd M, with $n = 0, \ldots, K-1$. We pair the neighboring terms, i.e.,

$$\sum_{M=0}^{N_p-1} \rho_0(M) e^{-\gamma_1\tau m_{\max}}$$

$$= \left[\sum_{\text{even}M} + \sum_{\text{odd}M} \right] \rho_0(M) e^{-\gamma_1\tau m_{\max}}$$

$$= \sum_{n=0}^{K-1} [\rho_0(2n) + \rho_0(2n+1)] e^{-2\gamma_1\tau(K-n-1)}. \quad (A58)$$

Since

$$\rho_0(2n) + \rho_0(2n+1) = \frac{2 + e^{-\Gamma\tau(2n+1)} - e^{-\Gamma\tau(2n+2)}}{1+e^{-\Gamma\tau}}, \quad (A59)$$

we obtain

$$\sum_{M=0}^{N_p-1} \rho_0(M) e^{-\gamma_1\tau m_{\max}}$$

$$= \sum_{n=0}^{K-1} \frac{2 - e^{-\Gamma\tau(2n+1)} + e^{-\Gamma\tau(2n+2)}}{1+e^{-\Gamma\tau}} e^{-2\gamma_1(K-n-1)\tau}$$

$$= \frac{e^{-2\gamma_1(K-1)\tau}}{1+e^{-\Gamma\tau}} \left[2\frac{e^{2K\gamma_1\tau}-1}{e^{2\gamma_1\tau}-1} \right.$$

$$\left. + e^{-\Gamma\tau}(1-e^{-\Gamma\tau})\frac{e^{2K(\gamma_1-\Gamma)\tau}-1}{e^{2(\gamma_1-\Gamma)\tau}-1} \right]. \quad (A60)$$

Substituting these results into Eq. (A54) for $\mathcal{P}_1$, we obtain Eq. (A62) in the limit of large N_p, and the net absorption spectrum is obtained as

$$Q(\omega) = 2A^2\text{Re}\{\mathcal{P}_2(\omega) - \mathcal{P}_1(\omega)\}$$
$$= 2A^2\text{Re}\{\mathcal{P}_3(\omega) - 2\mathcal{P}_1(\omega)\}, \qquad (A61)$$

with the explicit analytical expressions for $\mathcal{P}_1$ and $\mathcal{P}_3$ given by Eqs. (A62) and (A51).

In the limit of large N_p (long times), the net absorption spectrum is simply proportional to N_p, in a way similar to Eq. (A51). Numerical calculations show that this limit is achieved within one to two spontaneous emission times, so that the further evolution of the spectrum is mostly limited to a linear increase of the amplitude with time, so that the spectrum can be characterized by the energy absorption rate per unit time. At shorter times, when the shape of the spectrum is still forming, the energy itself should be considered.

$$\mathcal{P}_1(\omega) = \frac{1}{(1+e^{-\Gamma\tau})\gamma_0} \left[\left(\frac{1-e^{-\Gamma\tau}}{\Gamma} - e^{-\gamma_0\tau}\frac{e^{\gamma_2\tau}-1}{\gamma_2} + \frac{e^{\gamma_2\tau}-1}{\gamma_2}\frac{1-e^{-\gamma_0\tau}}{e^{2\gamma_1\tau}-1} \right) \left(N_p + \frac{e^{-\Gamma\tau}}{1+e^{-\Gamma\tau}} \right) \right.$$

$$\left. - \frac{e^{\gamma_2\tau}-1}{\gamma_2}\frac{1-e^{-\gamma_0\tau}}{e^{2\gamma_1\tau}-1} \left(2\frac{e^{-N_p\gamma_1\tau}-1}{e^{-2\gamma_1\tau}-1} + (e^{-\Gamma\tau} - e^{-2\Gamma\tau})\frac{e^{-N_p\gamma_1\tau}}{e^{-2\gamma_1\tau}-e^{-2\Gamma\tau}} \right) \right]. \qquad (A62)$$

In Fig. 7 we show a comparison of the numerical result and the analytical result described above for the absorption spectrum of a two-level system with detuning $\Delta = 3.0$ driven by a periodic pulse sequence of period $\tau = 0.2$ after 20 pulses. The comparison reveals very good agreement between the solutions, and the agreement indeed improves as the number of pulses increases.

---

[1] H. J. Kimble, Nature (London) **453**, 1023 (2008).

[2] A. Imamoğlu, D. D. Awschalom, G. Burkard, D. P. DiVincenzo, D. Loss, M. Sherwin, and A. Small, Phys. Rev. Lett. **83**, 4204 (1999).

[3] L. Childress, J. M. Taylor, A. S. Sørensen, and M. D. Lukin, Phys. Rev. Lett. **96**, 070504 (2006).

[4] R. Hanson and D. D. Awschalom, Nature (London) **453**, 1043 (2008).

[5] H. Bernien, B. Hensen, W. Pfaff, G. Koolstra, M. S. Blok, L. Robledo, T. H. Taminiau, M. Markham, D. J. Twitchen, L. Childress, and R. Hanson, Nature (London) **497**, 86 (2013).

[6] W. Pfaff, B. J. Hensen, H. Bernien, S. B. van Dam, M. S. Blok, T. H. Taminiau, M. J. Tiggelman, R. N. Schouten, M. Markham, D. J. Twitchen, and R. Hanson, Science **345**, 532 (2014).

[7] W. B. Gao, P. Fallahi, E. Togan, A. Delteil, Y. S. Chin, J. Miguel-Sanchez, and A. Imamoğlu, Nat. Commun. **4**, 2744 (2013).

[8] B. Hensen, H. Bernien, A. E. Dréau, A. Reiserer, N. Kalb, M. S. Blok, J. Ruitenberg, R. F. L. Vermeulen, R. N. Schouten, C. Abellán, W. Amaya, V. Pruneri, M. W. Mitchell, M. Markham, D. J. Twitchen, D. Elkouss, S. Wehner, T. H. Taminiau, and R. Hanson, Nature (London) **526**, 682 (2015).

[9] L. C. Bassett, F. J. Heremans, C. G. Yale, B. B. Buckley, and D. D. Awschalom, Phys. Rev. Lett. **107**, 266403 (2011).

[10] A. Faraon, P. E. Barclay, C. Santori, K.-M. C. Fu, and R. G. Beausoleil, Nat. Photonics **5**, 301 (2011).

[11] M. W. Doherty, N. B. Manson, P. Delaney, F. Jelezko, J. Wrachtrup, and L. C. L. Hollenberg, Phys. Rep. **528**, 1 (2013).

[12] A. Sipahigil, K. D. Jahnke, L. J. Rogers, T. Teraji, J. Isoya, A. S. Zibrov, F. Jelezko, and M. D. Lukin, Phys. Rev. Lett. **113**, 113602 (2014).

[13] L. J. Rogers, K. D. Jahnke, M. H. Metsch, A. Sipahigil, J. M. Binder, T. Teraji, H. Sumiya, J. Isoya, M. D. Lukin, P. Hemmer, and F. Jelezko, Phys. Rev. Lett. **113**, 263602 (2014).

[14] C. Santori, D. Fattal, J. Vučković, G. S. Solomon, and Y. Yamamoto, Nature (London) **419**, 594 (2002).

[15] S. G. Carter, T. M. Sweeney, M. Kim, C. S. Kim, D. Solenov, S. E. Economou, T. L. Reinecke, L. Yang, A. S. Bracker, and D. Gammon, Nat. Photonics **7**, 329 (2013).

[16] K.-M. C. Fu, C. Santori, P. E. Barclay, L. J. Rogers, N. B. Manson, and R. G. Beausoleil, Phys. Rev. Lett. **103**, 256404 (2009).

[17] W. P. Ambrose and W. E. Moerner, Nature (London) **349**, 225 (1991).

[18] J. Hansom, C. H. H. Schulte, C. Matthiesen, M. J. Stanley, and M. Atatüre, Appl. Phys. Lett. **105**, 172107 (2014).

[19] V. M. Acosta, C. Santori, A. Faraon, Z. Huang, K.-M. C. Fu, A. Stacey, D. A. Simpson, K. Ganesan, S. Tomljenovic-Hanic, A. D. Greentree, S. Prawer, and R. G. Beausoleil, Phys. Rev. Lett. **108**, 206401 (2012).

[20] A. V. Kuhlmann, J. Houel, A. Ludwig, L. Greuter, D. Reuter, A. D. Wieck, M. Poggio, and R. J. Warburton, Nat. Phys. **9**, 570 (2013).

[21] S. A. Crooker, J. Brandt, C. Sandfort, A. Greilich, D. R. Yakovlev, D. Reuter, A. D. Wieck, and M. Bayer, Phys. Rev. Lett. **104**, 036601 (2010).

[22] C. Matthiesen, M. J. Stanley, M. Hugues, E. Clarke, and M. Atatüre, Sci. Rep. **4**, 4911 (2014).

[23] H. F. Fotso, A. E. Feiguin, D. D. Awschalom, and V. V. Dobrovitski, Phys. Rev. Lett. **116**, 033603 (2016).

[24] A. Lenhard, M. Bock, C. Becher, S. Kucera, J. Brito, P. Eich, P. Müller, and J. Eschner, Phys. Rev. A **92**, 063827 (2015).

[25] N. Trautmann and G. Alber, Phys. Rev. A **93**, 053807 (2016).

[26] S. Yang, Y. Wang, D. D. Bhaktavatsala Rao, T. H. Tran, A. S. Momenzadeh, M. Markham, D. J. Twitchen, P. Wang, W. Yang, R. Stöhr, P. Neumann, H. Kosaka, and J. Wrachtrup, Nat. Photonics **10**, 507 (2016).

[27] A. Einstein, Phys. Z. **18**, 121 (1917).

[28] B. R. Mollow, Phys. Rev. A **5**, 2217 (1972).

[29] F. Y. Wu, S. Ezekiel, M. Ducloy, and B. R. Mollow, Phys. Rev. Lett. **38**, 1077 (1977).

[30] C. Cohen-Tannoudji, J. Dupont-Roc, and G. Grynberg, *Atom-Photon Interactions, Basic Processes and Applications* (Wiley, New York, 1992).

[31] B. R. Mollow, Phys. Rev. A **5**, 1522 (1972).

[32] M. O. Scully and M. S. Zubairy, *Quantum Optics* (Cambridge University Press, New York, 1997).

[33] I. M. Mirza and S. J. van Enk, Phys. Rev. A **90**, 043831 (2014).

[34] I. M. Mirza, S. J. van Enk, and H. J. Kimble, J. Opt. Soc. Am. B **30**, 2640 (2013).

[35] J. H. Eberly and K. Wódkiewicz, J. Opt. Soc. Am. B **67**, 1252 (1977).

[36] B. R. Mollow, Phys. Rev. **188**, 1969 (1969).

[37] S. H. Autler and C. H. Townes, Phys. Rev. **100**, 703 (1955).

[38] P. L. Knight and P. W. Milonni, Phys. Rep. **66**, 21 (1980).

[39] W. Heitler, *The Quantum Theory of Radiation*, 3rd ed. (Oxford University Press, London, 1960).

[40] R. Loudon, *The Quantum Theory of Light* (Clarendon, Oxford, 1983).

[41] S. Bloom and H. Margenau, Phys. Rev. **90**, 791 (1953).